

RETRIEVAL OF CO COLUMN ABUNDANCE IN THE MARTIAN THERMOSPHERE FROM FUV DISK OBSERVATIONS BY EMM EMUS

J. S. Evans, J. Correira, Computational Physics, Inc (CPI), Springfield, VA, USA (evans@cpi.com), **J. Deighan, S. Jain**, Laboratory for Atmospheric and Space Physics (LASP) at University of Colorado, Boulder, CO, USA, **H. Almatroushi**, Mohammed Bin Rashid Space Center (MBRSC), Dubai, UAE, **H. Almazmi**, United Arab Emirates Space Agency, Abu Dhabi, UAE, **M. Chaffin**, Laboratory for Atmospheric and Space Physics (LASP) at University of Colorado, Boulder, CO, USA, **S. England**, Virginia Polytechnic Institute and State University, Aerospace and Ocean Engineering, Blacksburg, VA, USA, **M. Fillingim**, Space Sciences Laboratory (SSL), University of California, Berkeley, CA, USA, **F. Forget**, Laboratoire de Météorologie Dynamique, Institut Pierre Simon Laplace Sorbonne Université, Paris, France, **G. Holsclaw**, Laboratory for Atmospheric and Space Physics (LASP) at University of Colorado, Boulder, CO, USA, **R. Lillis**, Space Sciences Laboratory (SSL), University of California, Berkeley, CA, USA, **F. Lootah**, Mohammed Bin Rashid Space Center (MBRSC), Dubai, UAE.

Introduction:

Carbon monoxide (CO) plays a major role in the chemical cycles of carbon dioxide (CO₂), hydrogen, and oxygen, and is a tracer of the thermal profile and winds in the Martian middle atmosphere. With a mean lifetime of about 6 Mars years (Krasnopolsky, 2007), CO is produced primarily through CO₂ photolysis in the middle atmosphere and is effectively lost in the lower atmosphere through catalysis by the OH radical produced by water vapor (H₂O) photolysis. Given such a long lifetime (relative to one Mars sol), no variation of CO with local time is expected. However, as an incondensable, CO is expected to vary both locally and temporally with Mars season. The spatial distribution of CO is therefore an important quantity that can be used to constrain models of photochemical and dynamical processes in the Martian atmosphere.

From its vantage point in orbit, the Emirates Ultraviolet Spectrometer (EMUS) onboard the Emirates Mars Mission (EMM) Hope probe (Amiri *et al.*, 2021) images Mars at extreme- and far-ultraviolet wavelengths extending from approximately 100 to 170 nm. The EMUS $\Sigma\text{CO}/\text{CO}_2$ algorithm (where Σ

indicates a slant path integral) provides a measure of relative composition variability within the Martian thermosphere by deriving the column abundance of CO above a fixed reference column density of CO₂ from EMUS images. The $\Sigma\text{CO}/\text{CO}_2$ algorithm traces its origins to the $\Sigma\text{O}/\text{N}_2$ algorithm used at Earth for studying relative variability in atomic oxygen abundance from remote sensing observations (Strickland *et al.*, 1995; Evans *et al.*, 1995; Correira *et al.*, 2021). In a similar manner, relative composition can be inferred for the Martian atmosphere using CO and CO₂.

Observations:

We use newly released data taken with EMUS aboard the EMM Hope probe to infer relative composition variability within the Martian thermosphere by deriving the column abundance of CO above a fixed reference column density of CO₂. The orbit of the EMM Hope probe has an apoapsis at 42,650 km and periapsis at 19,970 km with a 54.5 hour period. This high altitude orbit affords a synoptic

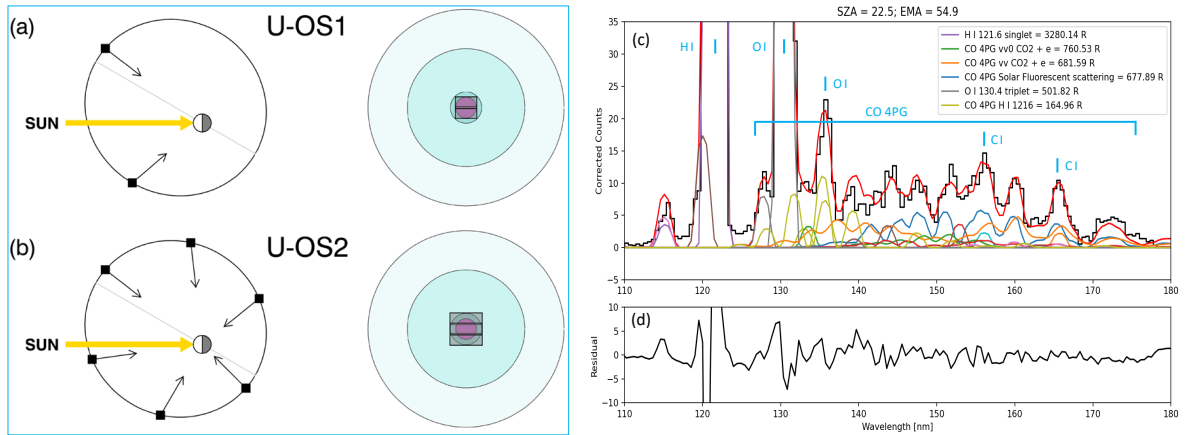


Figure 1. (a) Left: Position of EMM in its orbit (square symbols) and lines of sight (arrows) relative to Mars and the Sun for U-OS1 observations. Right: Observation mode from the perspective of EMM, with the area scanned by the 10.75° tall instrument slit (grey rectangles) overlaid on Mars. (b) Same as (a) but for U-OS2 observations. (c) EMUS spectrum measured on April 24, 2021 shown in black with multiple linear regression (MLR) fit shown in red. (d) The difference (counts/bin) between the measured spectrum and MLR total fit.

view of Mars with full local time coverage every 9-10 days (Holsclaw *et al.*, 2021). High and low resolution slits have angular widths of 0.18° and 0.25° and spectral widths of 1.3 nm and 1.8 nm, respectively (Holsclaw *et al.*, 2021). EMUS remotely senses the thermosphere at 100 – 200 km altitude, observing far-ultraviolet (FUV) emissions (see Figure 1) from hydrogen (H I 121.6 nm), oxygen (O I 130.4 and 135.6 nm), and carbon monoxide (CO 4PG 140 – 170 nm). The first data release, covering February 10, 2021 to May 23, 2021, was delivered in early October 2021. For the present analysis, we utilize EMUS U-OS1 and U-OS2 disk observations covering February 20, 2021 to March 18, 2022.

Retrieval Algorithm:

The $\Sigma\text{CO}/\text{CO}_2$ algorithm uses a lookup table approach by first generating a series of model atmospheres that span the expected range of physically realistic atmospheres. When used with EMUS observations, the lookup table provides a unique mapping from intensity to CO/CO_2 column density ratio for a given solar zenith angle (SZA) and emission angle (EMA). Intensities from the optically allowed CO Fourth Positive Group (4PG) band system ($A^1\Pi \rightarrow X^1\Sigma^+$) are used as a signature of CO variability.

Results:

EMUS Level 3 data files contain $\Sigma\text{CO}/\text{CO}_2$ derived from EMUS observations. The algorithm is primarily intended for U-OS1 observations, though it may be applied to U-OS2 observations as well, or any EMUS observation that views the disk of Mars. We note that the spatial resolution for other EMUS observation types is typically too coarse to derive useful data products. U-OS1 is comprised of two scans, each scan imaging a little more than half the Martian disk visible from EMUS' vantage point. U-OS2 observations consist of three scans, with one scan covering approximately 2/3 of the Martian disk, while the first and last scans cover the edges of the disk (see Figure 1). Before ingestion by the $\Sigma\text{CO}/\text{CO}_2$ algorithm, Level 2 data may be spatially binned to increase signal to noise.

Figures 2 and 3 present EMUS data. Figure 2 shows the SZA and the intensity of CO 4PG excited by solar Lyman α photons on the left and right, respectively. The upper row shows values for the central swath of an U-OS2 observation from April 24, 2021, while the bottom row shows the central swath from an U-OS2 observation on June 18, 2021. The left column of Figure 3 shows $\Sigma\text{CO}/\text{CO}_2$ derived from the algorithm, while the right hand column shows the percent difference of each pixel from the mean swath value. Uncertainty values are reported for the input intensities and derived $\Sigma\text{CO}/\text{CO}_2$ and are separated into random, systematic, and model uncertainties (the

latter uncertainty does not apply to the input radiances). A rigorous propagation of errors is used, beginning with the intensity uncertainties present in Level 2B data.

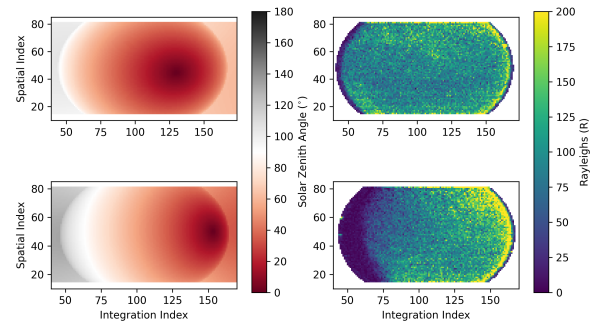


Figure 2. Solar zenith angles (left) and solar Lyman α pumped CO 4PG intensity (right) for the second swath (out of three) for U-OS2 observations on April 24, 2021 (top row) and June 18, 2021 (bottom row).

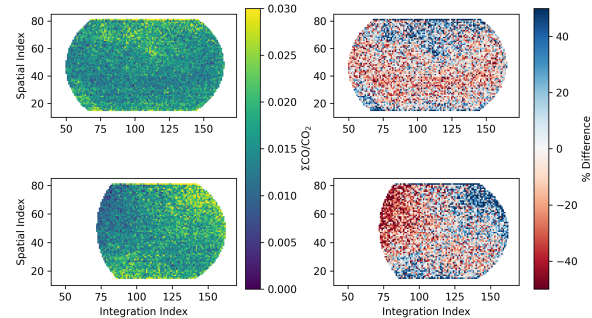


Figure 3. Retrieved $\Sigma\text{CO}/\text{CO}_2$ (left) and percent difference from swath averaged $\Sigma\text{CO}/\text{CO}_2$ (right) for the same observations shown in Figure 2.

References:

- Amiri, H.E. S., *et al.*, The Emirates Mars Mission. *Space Sci. Rev.*, 218, 4 (2021).
- Correia, J., Evans, J. S., *et al.*, Thermospheric Composition and Solar EUV Flux From the Global-Scale Observations of the Limb and Disk (GOLD) Mission. *J. Geophys. Res.*, 126 (12), e29517 (2021).
- Evans, J. S., *et al.*, Satellite remote sensing of thermospheric O/N₂ and solar EUV. 2: Data analysis. *J. Geophys. Res.*, 100, 12227 (1995).
- Holsclaw, G. M., *et al.*, The Emirates Mars Spectrometer (EMUS) for the EMM Mission. *Space Sci. Rev.*, 217, 79 (2021).
- Krasnopolsky, V. A. Long-term spectroscopic observations of Mars using IRTF/CSHELL: Mapping of O₂ dayglow, CO, and search for CH₄. *Icarus*, 190, no. 1 (2007).
- Strickland, D. J., Evans, J. S., *et al.*, Satellite remote sensing of thermospheric O/N₂ and solar EUV. 1: Theory. *J. Geophys. Res.*, 100, 12217 (1995).